



## Realization of semiconducting Cu<sub>2</sub>Se by direct selenization of Cu(111)

Yumu Yang(杨雨沐), Qilong Wu(吴奇龙), Jiaqi Deng(邓嘉琦), Jing Wang(王静), Yu Xia(夏雨), Xiaoshuai Fu(富晓帅), Qiwei Tian(田麒玮), Li Zhang(张力), Long-Jing Yin(殷隆晶), Yuan Tian(田园), Sheng-Yi Xie(谢声意), Lijie Zhang(张利杰), and Zhihui Qin(秦志辉)

**Citation:** Chin. Phys. B, 2021, 30 (11): 116802. DOI: 10.1088/1674-1056/ac0037

Journal homepage: <http://cpb.iphy.ac.cn>; <https://iopscience.iop.org/cpb>

### What follows is a list of articles you may be interested in

---

## Phase transition-induced superstructures of $\beta$ -Sn films with atomic-scale thickness

Le Lei(雷乐), Feiyue Cao(曹飞跃), Shuya Xing(邢淑雅), Haoyu Dong(董皓宇), Jianfeng Guo(郭剑锋), Shangzhi Gu(顾尚志), Yanyan Geng(耿燕燕), Shuo Mi(米烁), Hanxiang Wu(吴翰翔), Fei Pang(庞斐), Rui Xu(许瑞), Wei Ji(季威), and Zhihai Cheng(程志海)

Chin. Phys. B, 2021, 30 (9): 096804. DOI: 10.1088/1674-1056/ac11e8

## NBN-doped nanographene embedded with five- and seven-membered rings on Au(111)

### surface

Huan Yang(杨欢), Yun Cao(曹云), Yixuan Gao(高艺璇), Yubin Fu(付钰彬), Li Huang(黄立), Junzhi Liu(刘俊治), Xinliang Feng(冯新亮), Shixuan Du(杜世萱), and Hong-Jun Gao(高鸿钧)

Chin. Phys. B, 2021, 30 (5): 056802. DOI: 10.1088/1674-1056/abeede

## Epitaxial growth of antimony nanofilms on HOPG and thermal desorption to control the

### film thickness

Shuya Xing(邢淑雅), Le Lei(雷乐), Haoyu Dong(董皓宇), Jianfeng Guo(郭剑峰), Feiyue Cao(曹飞跃), Shangzhi Gu(顾尚志), Sabir Hussain, Fei Pang(庞斐), Wei Ji(季威), Rui Xu(许瑞), Zhihai Cheng(程志海)

Chin. Phys. B, 2020, 29 (9): 096801. DOI: 10.1088/1674-1056/aba27c

## STM study of selenium adsorption on Au(111) surface

Bin Liu(刘斌), Yuan Zhuang(庄源), Yande Que(阙炎德), Chaoqiang Xu(徐超强), Xudong Xiao(肖旭东)

Chin. Phys. B, 2020, 29 (5): 056801. DOI: 10.1088/1674-1056/ab821d

## Triphenylene adsorption on Cu(111) and relevant graphene self-assembly

Qiao-Yue Chen(陈乔悦), Jun-Jie Song(宋俊杰), Liwei Jing(井立威), Kaikai Huang(黄凯凯), Pimo He(何丕模), Hanjie Zhang(张寒洁)

Chin. Phys. B, 2020, 29 (2): 026801. DOI: 10.1088/1674-1056/ab6583

---

# Realization of semiconducting Cu<sub>2</sub>Se by direct selenization of Cu(111)\*

Yumu Yang(杨雨沐), Qilong Wu(吴奇龙), Jiaqi Deng(邓嘉琦), Jing Wang(王静), Yu Xia(夏雨), Xiaoshuai Fu(富晓帅), Qiwei Tian(田麒玮), Li Zhang(张力), Long-Jing Yin(殷隆晶), Yuan Tian(田园), Sheng-Yi Xie(谢声意), Lijie Zhang(张利杰)<sup>†</sup>, and Zhihui Qin(秦志辉)<sup>‡</sup>

Key Laboratory for Micro/Nano Optoelectronic Devices of Ministry of Education & Hunan Provincial Key Laboratory of Low-Dimensional Structural Physics and Devices, School of Physics and Electronics, Hunan University, Changsha 410082, China

(Received 28 April 2021; revised manuscript received 6 May 2021; accepted manuscript online 12 May 2021)

Bulk group IB transition-metal chalcogenides have been widely explored due to their applications in thermoelectrics. However, a layered two-dimensional form of these materials has been rarely reported. Here, we realize semiconducting Cu<sub>2</sub>Se by direct selenization of Cu(111). Scanning tunneling microscopy measurements combined with first-principles calculations allow us to determine the structural and electronic properties of the obtained structure. X-ray photoelectron spectroscopy data reveal chemical composition of the sample, which is Cu<sub>2</sub>Se. The observed moiré pattern indicates a lattice mismatch between Cu<sub>2</sub>Se and the underlying Cu(111)- $\sqrt{3} \times \sqrt{3}$  surface. Differential conductivity obtained by scanning tunneling spectroscopy demonstrates that the synthesized Cu<sub>2</sub>Se exhibits a band gap of 0.78 eV. Furthermore, the calculated density of states and band structure demonstrate that the isolated Cu<sub>2</sub>Se is a semiconductor with an indirect band gap of  $\sim 0.8$  eV, which agrees quite well with the experimental results. Our study provides a simple pathway varying toward the synthesis of novel layered 2D transition chalcogenides materials.

**Keywords:** Cu<sub>2</sub>Se, scanning tunneling microscopy, scanning tunneling spectroscopy, semiconducting, selenization

**PACS:** 68.37.Ef, 71.15.Mb

**DOI:** 10.1088/1674-1056/ac0037

## 1. Introduction

The discovery of graphene ignited the research of other two-dimensional (2D) materials with exotic properties.<sup>[1–4]</sup> For instance, elemental 2D materials such as silicene,<sup>[5–7]</sup> germanene,<sup>[8–13]</sup> stanene<sup>[14]</sup> and bismuthene<sup>[15]</sup> are predicted to exhibit quantum spin Hall effect, which would have application in low-power electronics to fault-tolerant quantum computing.<sup>[16]</sup> Transition metal dichalcogenides (TMDs) are typical 2D materials with intriguing properties like tunable bandgaps and inherently stronger spin–orbit coupling, which can be exploited for various device applications.<sup>[17–20]</sup> Bulk group IB transition metal chalcogenides are well known for their thermoelectric properties especially the application for solar cells materials.<sup>[21]</sup> Recently, 2D form of group IB transition metal chalcogenides starts to receive attention although their bulk parent materials are not layered. Shah *et al.*<sup>[22]</sup> confirmed the formation of honeycomb structure of AgTe, and Ünzelmann *et al.*<sup>[23]</sup> found experimentally the Rashba-type spin splitting in different bands of AgTe related to the existence of orbital angular momentum. CuSe is a fascinating transition metal monochalcogenide that has been calculated to host the Dirac nodal line fermion, protected by mirror reflection

symmetry.<sup>[24]</sup> It has been reported that CuSe can be grown on Cu(111).<sup>[25]</sup> However, the fabricated monolayer CuSe shows varying features, such as, with intrinsic nanopores<sup>[25]</sup> and in 1D moiré pattern.<sup>[24,26]</sup> Walen *et al.* systemically investigated low coverage of Se on Cu(111) forming variable overlayer structures.<sup>[27]</sup> Cu<sub>2</sub>Se has long been known to be an excellent thermoelectric material serving as energy storage. It is also quite important for the synthesis of a class of thin film solar cells, Cu(In, Ga)Se<sub>2</sub> (CIGS).<sup>[28]</sup> Layered structure of Cu<sub>2</sub>Se was raised recently.<sup>[29]</sup> Previous reports have shown the fabrication of Cu<sub>2</sub>Se by co-evaporation of Cu and Se and found the phase transformation with pure thermo driven.<sup>[30]</sup> Wang *et al.* developed a straightforward way to synthesis PtSe<sub>2</sub> by direct selenization of Pt(111).<sup>[31]</sup> Based on this strategy, a few reports have shown the feasibility of fabricating new layered structures without layered bulk counterpart.<sup>[32–34]</sup> With this regards, direct selenization of Cu to form Cu<sub>2</sub>Se has not been reported yet.

Here, we report the synthesis of large-scale monolayer Cu<sub>2</sub>Se by direct selenization of Cu(111). Scanning tunneling microscopy and spectroscopy (STM/STS) were employed to explore its structural and electronic properties. X-ray pho-

\*Project supported by the National Natural Science Foundation of China (Grant Nos. 51772087, 11904094, 51972106, and 11804089), the Strategic Priority Research Program of Chinese Academy of Sciences (Grant No. XDB30000000), and Natural Science Foundation of Hunan Province, China (Grant Nos. 2019JJ50034 and 2019JJ50073).

<sup>†</sup>Corresponding author. E-mail: [lijiezhang@hnu.edu.cn](mailto:lijiezhang@hnu.edu.cn)

<sup>‡</sup>Corresponding author. E-mail: [zhqin@hnu.edu.cn](mailto:zhqin@hnu.edu.cn)

toelectron spectroscopy (XPS) data reveals the composition of the sample as  $\text{Cu}_2\text{Se}$ . First-principles calculations indicate monolayer semiconductor  $\text{Cu}_2\text{Se}$  with an indirect band gap of 0.8 eV, which agrees quite well with the STS measurement.

## 2. Experimental and theory details

The sample was fabricated by physical vapor deposition of Se on Cu(111) in a ultrahigh vacuum (UHV) chamber equipped with an STM (Unisoku). The base pressure of the system is below  $2.0 \times 10^{-10}$  mbar. Prior to the Se deposition, Cu(111) (purchased from MaTeck) was cleaned via cycles of argon-ion (1.2  $\mu\text{A}$ , 1 kV) sputtering followed by annealing at  $\sim 550^\circ\text{C}$ . Molecular beams of Se (99.999%, Alfa Aesar) were deposited onto the clean Cu(111) surface from a home-built evaporator. During the evaporation the substrate was kept at room temperature whereas the pressure of the vacuum chamber went to  $10^{-7}$  mbar. We calibrated the Se deposition rate by checking the condition of overlayer coverage on Cu(111) surface. Here, in our experiment, more than one monolayer amount of Se has been deposited on the substrate. All the STM measurements were performed at room temperature. Differential conductance ( $dI/dV$ ) spectra were acquired by a standard lock-in amplifier at a frequency of 973 Hz with a 50 mV modulation. The tip calibration was performed on an Au(111) substrate.

The calculations were performed within the projected augmented wave formalism<sup>[35]</sup> as implemented in the Vienna *ab-initio* simulation package (VASP).<sup>[36,37]</sup> To calculate the electronic structure of  $\text{Cu}_2\text{Se}$ , we used the GW scheme.<sup>[38]</sup> The initial Green's functions were calculated using density functional theory (DFT) within the generalized gradient approximation,<sup>[39]</sup> and self-consistently iterated four times, which is sufficient to achieve numerical convergence. The screened Coulomb interaction was calculated at the full RPA level, and not updated during the calculation. To this end, we performed a numerical integration over the frequency axis with 50 grid points. In the calculation of the quasiparticle energies, both diagonal and off-diagonal elements of the self-energy matrix were considered. In all calculations, we used an energy cutoff of 400 eV for the plane-waves, and a convergence threshold of  $10^{-8}$  eV. The number of unoccupied states in GW calculations was set to 700 per unit cell, which spans an energy interval of around 90 eV. The Brillouin zone was sampled by a  $(4 \times 4)$   $k$ -point mesh. In order to avoid spurious interactions between the  $\text{Cu}_2\text{Se}$  layers in the nonperiodic direction, a 30 Å thick vacuum slab was added in the direction normal to the  $\text{Cu}_2\text{Se}$  layer. The crystal structure of  $\text{Cu}_2\text{Se}$  was adopted from Ref. [30], with the lattice constant 4.0 Å. We checked that the numerical parameters ensure that the quasiparticle gap is accurate to within 10 meV.

## 3. Results and discussion

A schematic sample preparation process is shown in Fig. 1(a). Prior to Se deposition, an atomic clean Cu(111) substrate is required. Large-scale empty state STM image of Cu(111) substrate is shown in Fig. 1(b). Clear Cu step edges are visible revealing the cleanness of the substrate. Afterwards, we deposited a few monolayers of Se on the substrate. The surface was dramatically modified and covered by full of protrusions (see Fig. 1(c)). We cannot get high resolution STM images at this condition since the unlikely formation of ordered structure without annealing. Subsequently, we annealed the sample mildly at a temperature of  $\sim 200^\circ\text{C}$  for 10 min. Figure 2(a) shows a large-scale STM image of the surface, which contains a few ordered structural terraces with hexagonal-like shape. The height difference of these terraces is  $\sim 0.2$  nm (see the line profile in the inset of Fig. 2(a)), which is in good consistence with the step height of Cu(111) single crystal. We zoom-in on a random position of the terrace (marked by a green square), a clear moiré pattern with a periodicity of 3.7 nm is visible. Further zoom-in small-scale atomic resolution STM image is shown in Fig. 2(c). A line profile indicates the periodicity of the structure, revealing the lattice constant of  $\sim 0.4$  nm. Fast Fourier transform (FFT), presented in the inset of Fig. 2(b) shows clear double periodicities, which agrees quite well with the measured ones.

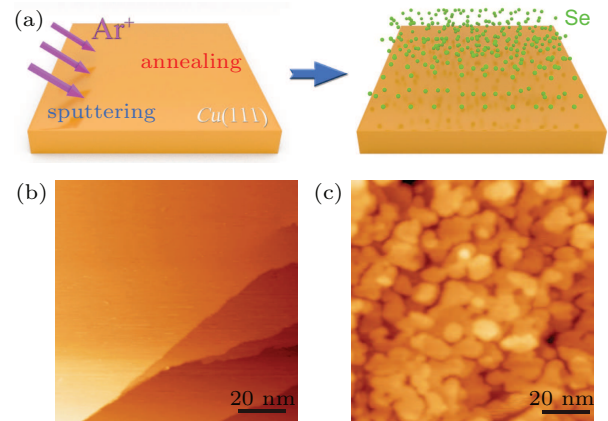


**Fig. 1.** Fabrication process of Cu(111) selenization. (a) Schematics of the substrate cleaning and Se deposition. (b) Large scale STM image of a clean Cu(111) (set points: sample bias 1 V and tunneling current 100 pA). (c) STM image of the surface after a few monolayers of Se deposited on the surface before annealing (scanning parameter: sample bias 1 V and tunneling current 2 pA).

Moiré pattern can be formed either by the lattice mismatch and/or the rotation of stacked periodic structure layers. We analyzed the relations of the hexagonal moiré pattern superstructure wavelength and the precise atomic lattice structure of the overlayer and found that the bottom layer should also be a hexagonal shape. The relation of the given lattice constants of the stacking layers  $a$  (top) and  $b$  (bottom), the relative rotation angle  $\phi$ , and the moiré wavelength  $\lambda$  can be

described as follow:<sup>[40]</sup>

$$\lambda = \frac{a^2}{\sqrt{a^2 - 2ab \cos \varphi + b^2}}. \quad (1)$$

Based on the top layer lattice constant and the periodicity of the moiré pattern, we calculate that the bottom layer should have the lattice constant of reconstructed  $\sqrt{3} \times \sqrt{3}$  Cu(111) i.e., 4.43 Å with the assumption that no twist can fit perfectly. We would like to mention here that the formation of  $\sqrt{3} \times \sqrt{3}$  reconstruction of Cu(111) is of common phenomenon for the deposition of Se on Cu(111).<sup>[27]</sup> In previous studies, less than one monolayer amount of Se deposited on Cu(111) showed a significant different feature, forming either nanoscale holes or 1D chains caused by the mismatch of the overlayer CuSe with the Cu(111) substrate.<sup>[24,25,41]</sup> The significant difference of the feature reflects the critical role of the amount of the Se deposition. A systemic study of low coverage Se on Cu(111) revealed the formation of 2D copper selenide on Cu(111).<sup>[27]</sup> To the best of our knowledge, all the previous studies have not shown a similar structure with what we found here.

Therefore, STS measurements were performed to explore the electronic properties of the synthetic overlayer. Figure 2(d) shows the distinctive differential conductivity ( $dI/dV$ ) spectra, recorded on top of the overlayer at different positions. According to the  $dI/dV$  curve, we deduce its conductive band minimum (CBM) and valence band maximum (VBM) at 0.70 eV and  $-0.08$  eV, respectively. These values altogether give a quasi-particle band gap of  $\sim 0.78$  eV. There is no obvious variation of all the  $dI/dV$  curves performed on other positions of the overlayer, revealing uniform electronic properties of the synthesized monolayer structure. The finding of semiconducting feature here is obviously different from the previous formed CuSe on Cu(111),<sup>[24]</sup> where combined DFT calculations and angle resolved photoemission spectroscopy (ARPES) measurements have revealed its metallic properties. Furthermore, our measured band gap is also significantly larger than the value obtained by Guo *et al.* on CuSe/Cu(111) recently.<sup>[41]</sup> Hence, we carefully exclude the possibility of forming CuSe in our case. Recently, a new layered structure of Cu<sub>2</sub>Se has been raised by Nguyen *et al.*<sup>[29]</sup> Based on the theoretical calculations, they found that the new structure of Cu<sub>2</sub>Se is energetically, dynamically and mechanically stable. Furthermore, they also found that Cu<sub>2</sub>Se has a band gap of 0.74 eV,<sup>[29]</sup> which is quite close with our experimental results. Because of these stability and layered nature, the newly proposed Cu<sub>2</sub>Se structure can be fabricated on substrate. With a careful scrutiny of the structural and electronic properties of the obtained structure, we find that this newly reported structure Cu<sub>2</sub>Se can fits our findings quite well. Interestingly, recently Qian *et al.* co-deposited Se and Cu in

ultra-high vacuum condition on bilayer graphene terminated of SiC substrate.<sup>[30]</sup> They proposed the synthesized structure as  $\lambda$ -phase of Cu<sub>2</sub>Se at room temperature. The top Se atoms were resolved by STM as a triangle/hexagonal shape.

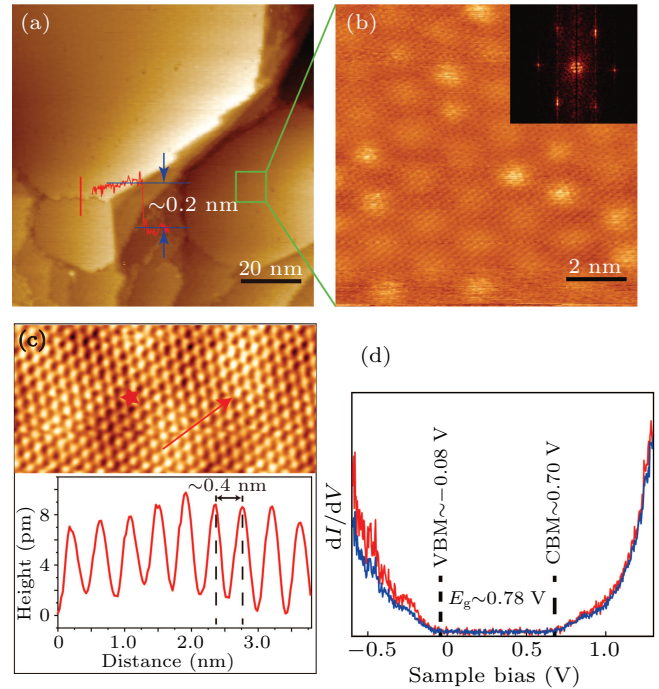


**Fig. 2.** The atomic structure and electronic properties of Cu<sub>2</sub>Se. (a) A large scale STM image (sample bias 1 V and tunneling current 10 pA) of Cu<sub>2</sub>Se. A line-profile across the step edge presented in the inset with a height of around 0.2 nm. (b) A zoom-in STM image (sample bias 700 mV and tunneling current 100 pA) of Cu<sub>2</sub>Se. Image inset is the FFT at (b). (c) Atomic configuration of Cu<sub>2</sub>Se at the top panel and the lower panel is the line-profile of Cu<sub>2</sub>Se. (d)  $dI/dV$  spectra of Cu<sub>2</sub>Se indicating a semiconducting feature with a band gap of 0.78 eV.

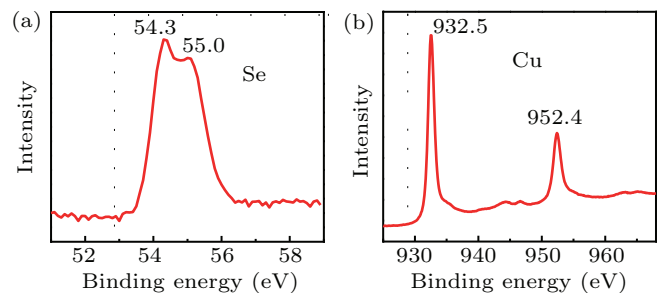


**Fig. 3.** The core level XPS spectrum of Cu<sub>2</sub>Se sample on Cu(111) substrate. (a) Two peaks can be resolved in the Se 3d signal, 54.3 eV and 55.0 eV. (b) Two well-defined peaks of Cu locate at 932.5 eV and 952.4 eV.

In order to further verify the composition of the synthesized sample, we performed x-ray photoelectron spectroscopy (XPS) on the surface. Monochromatic radiation light was realized by four high resolution gratings and controlled by a hemispherical energy analyzer that possesses a photon energy in the range from 10 eV to 1100 eV. High-resolution XPS spectra of Cu 2p and Se 3d regions are plotted in Figs. 3(a) and 3(b). The binding energies of Cu 2p<sub>3/2</sub> and Cu 2p<sub>1/2</sub> are 932.5 eV and 952.4 eV, respectively. It demonstrates that the 932.5 eV peak can be ascribed to Cu<sup>+</sup> ions.<sup>[42]</sup> In addition, compared with

the XPS data of  $\text{Cu}_{2-x}\text{Se}$ , the binding energy peak position of Se  $3d_{5/2}$  in our case is quite different.<sup>[43]</sup> However, our results are in good agreement with the XPS data of  $\text{Cu}_2\text{Se}$  reported recently,<sup>[30,44]</sup> revealing that the composition of the sample is indeed  $\text{Cu}_2\text{Se}$ .

First-principles GW calculations were carried out to further clarify the electronic properties of the synthesized  $\text{Cu}_2\text{Se}$ . Figures 4(a) and 4(b) show ball and stick models of top and side views of  $\text{Cu}_2\text{Se}$ , where yellow balls represent Se atoms and brown ones are Cu atoms. The model was inspired by Ref. [30], from which we adopt the  $\lambda$ -phase of  $\text{Cu}_2\text{Se}$ . In the calculation, we consider an isolated monolayer  $\lambda$ - $\text{Cu}_2\text{Se}$  and investigate its electronic properties. The calculated project density of state reveals an indirect band gap of  $\sim 0.8$  eV, which is in accordance with our STS measurement of 0.78 eV. Deviation of the band gap between the theoretical calculation and the experimental results can be attributed to the Cu(111) substrate screening, which is neglected in our calculations. Therefore, the calculations provide additional evidences regarding the fabrication of monolayer  $\text{Cu}_2\text{Se}$ .

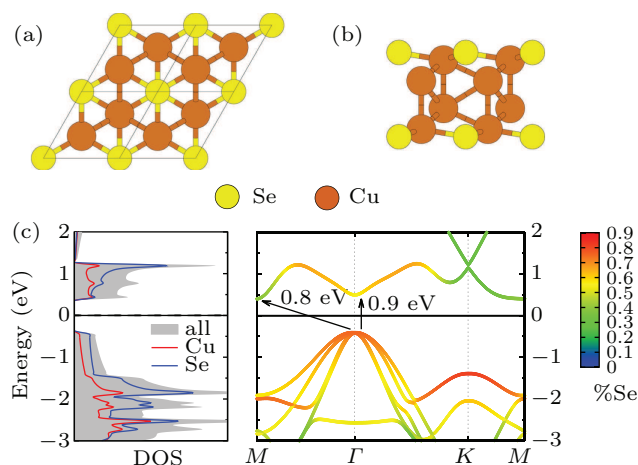


**Fig. 4.** First-principles GW calculations of monolayer  $\text{Cu}_2\text{Se}$ . (a) Top and (b) side views of monolayer  $\text{Cu}_2\text{Se}$  structure. (c) Density of states (DOS) and band structure calculated in this work within the GW0 scheme for monolayer  $\text{Cu}_2\text{Se}$ . Red and blue lines in DOS correspond to the contributions of Cu and Se states, respectively. The color bar indicates the contribution of Se states in the band structure.

## 4. Conclusion

In summary, we deposited a few monolayers Se on Cu(111) to form  $\text{Cu}_2\text{Se}$ , a new layered 2D transition metal chalcogenide material. Combining STM/STS, XPS and the first-principles calculations, we confirmed the synthesized overlayer of  $\text{Cu}_2\text{Se}$ . Differential conductivity reveals the semiconducting properties. The formed moiré pattern originates from the mismatch of  $\text{Cu}_2\text{Se}$  overlayer and underlayer Cu(111) but no moiré potential related electronic states were found. First-principles calculations verified the semiconducting properties which agrees quite well with scanning tunneling spectroscopy

results. This work indicates the successful synthesis of  $\text{Cu}_2\text{Se}$  by direct selenization of Cu(111), which paves a way of the fabrication of group IB transition metal chalcogenides.

## References

- [1] Novoselov K S, Geim A K, Morozov S V, Jiang D, Zhang Y, Dubonos S V, Grigorieva I V and Firsov A A 2004 *Science* **306** 666
- [2] Xing S, Lei L, Dong H, Guo J, Cao F, Gu S, Hussain S, Pang F, Ji W, Xu R and Cheng Z 2020 *Chin. Phys. B* **29** 096801
- [3] Fan P, Zhang R Z, Qi J, Li E, Qian G J, Chen H, Wang D F, Zheng Q, Wang Q, Lin X, Zhang Y Y, Du S, Hofer W A and Gao H J 2020 *Chin. Phys. B* **29** 098102
- [4] Dong L, Wang A W, Li E, Wang Q, Li G, Huan Q and Gao H J 2019 *Chin. Phys. Lett.* **36** 028102
- [5] Feng B, Ding Z, Meng S, Yao Y, He X, Cheng P, Chen L and Wu K 2012 *Nano Lett.* **12** 3507
- [6] Vogt P, De Padova P, Quaresima C, Avila J, Frantzeskakis E, Asensio M C, Resta A, Ealet B and Le Lay G 2012 *Phys. Rev. Lett.* **108** 155501
- [7] Wu Z B, Zhang Y Y, Li G, Du S and Gao H J 2018 *Chin. Phys. B* **27** 077302
- [8] Li L, Lu S Z, Pan J, Qin Z, Wang Y Q, Wang Y, Cao G Y, Du S and Gao H J 2014 *Adv. Mater.* **26** 4820
- [9] Zhang L, Bampoulis P, Rudenko A N, Yao Q, van Houselt A, Poelsema B, Katsnelson M I and Zandvliet H J W 2016 *Phys. Rev. Lett.* **116** 256804
- [10] Deng J, Ablat G, Yang Y, Fu X, Wu Q, Li P, Zhang L, Safaei A, Zhang L and Qin Z 2021 *J. Phys.: Condens. Matter* **33** 225001
- [11] Qin Z, Pan J, Lu S, Shao Y, Wang Y, Du S, Gao H J and Cao G 2017 *Adv. Mater.* **29** 1606046
- [12] Acun A, Zhang L, Bampoulis P, Farmanbar M, van Houselt A, Rudenko A N, Lingenfelder M, Brocks G, Poelsema B, Katsnelson M I and Zandvliet H J W 2015 *J. Phys.: Condens. Matter* **27** 443002
- [13] Qin Z H 2017 *Acta Phys. Sin.* **66** 216802 (in Chinese)
- [14] Zhu F F, Chen W J, Xu Y, Gao C L, Guan D D, Liu C H, Qian D, Zhang S C and Jia J F 2015 *Nat. Mater.* **14** 1020
- [15] Reis F, Li G, Dudy L, Bauernfeind M, Glass S, Hanke W, Thomale R, Schafer J and Claessen R 2017 *Science* **357** 287
- [16] Molle A, Goldberger J, Houssa M, Xu Y, Zhang S C and Akinwande D 2017 *Nat. Mater.* **16** 163
- [17] Wang Q H, Kalantar-Zadeh K, Kis A, Coleman J N and Strano M S 2012 *Nat. Nanotechnol.* **7** 699
- [18] Fu Q, Han J, Wang X, Xu P, Yao T, Zhong J, Zhong W, Liu S, Gao T, Zhang Z, Xu L and Song B 2020 *Adv. Mater.* **33** 1907818
- [19] Wu Q, Fu X, Yang K, Wu H, Liu L, Zhang L, Tian Y, Yin L J, Huang W Q, Zhang W, Wong P K J, Zhang L, Wee A T S and Qin Z 2021 *ACS Nano* **15** 4481
- [20] Guo Q M and Qin Z H 2021 *Acta Phys. Sin.* **70** 028101 (in Chinese)
- [21] Zhang Y, Wang Y, Xi L, Qiu R, Shi X, Zhang P and Zhang W 2014 *J. Chem. Phys.* **140** 074702
- [22] Shah J, Sohail H M, Uhrberg R I G and Wang W 2020 *J. Phys. Chem. Lett.* **11** 1609
- [23] Unzelmann M, Bentmann H, Eck P, Kisslinger T, Geldiyev B, Rieger J, Moser S, Vidal R C, Kissner K, Hammer L, Schneider M A, Fauster T, Sangiovanni G, Di Sante D and Reinert F 2020 *Phys. Rev. Lett.* **124** 176401
- [24] Gao L, Sun J T, Lu J C, Li H, Qian K, Zhang S, Zhang Y Y, Qian T, Ding H, Lin X, Du S and Gao H J 2018 *Adv. Mater.* **30** 1707055
- [25] Lin X, Lu J C, Shao Y, et al. 2017 *Nat. Mater.* **16** 717
- [26] Guo Q, Zhong Y, Huang M, Lu S and Yu Y 2020 *Thin Solid Films* **693** 137709
- [27] Walen H, Liu D J, Oh J, Yang H J, Kim Y and Thiel P A 2016 *Chemphyschem* **17** 2137
- [28] Nishimura T, Toki S, Sugiura H, Nakada K and Yamada A 2016 *Appl. Phys. Express* **9** 092301
- [29] Nguyen M C, Choi J H, Zhao X, Wang C Z, Zhang Z and Ho K M 2013 *Phys. Rev. Lett.* **111** 165502
- [30] Qian K, Gao L, Chen X, et al. 2020 *Adv. Mater.* **32** 1908314
- [31] Wang Y, Li L, Yao W, Song S, Sun J, Pan J, Ren X, Li C, Okunishi E and Wang Y Q 2015 *Nano Lett.* **15** 4013
- [32] Zhang S, Song Y, Li J M, Wang Z, Liu C, Wang J O, Gao L, Lu J C, Zhang Y Y, Lin X, Pan J, Du S X and Gao H J 2020 *Chin. Phys. B* **29** 077301

- [33] Liu B, Zhuang Y, Que Y, Xu C and Xiao X 2020 *Chin. Phys. B* **29** 056801
- [34] Sun H, Liang Z, Shen K, Luo M, Hu J, Huang H, Zhu Z, Li Z, Jiang Z and Song F 2018 *Appl. Surf. Sci.* **428** 623
- [35] Blöchl P E 1994 *Phys. Rev. B* **50** 17953
- [36] Kresse G and Furthmüller J 1996 *Phys. Rev. B* **54** 11169
- [37] Kresse G and Joubert D 1999 *Phys. Rev. B* **59** 1758
- [38] Shishkin M and Kresse G 2007 *Phys. Rev. B* **75** 235102
- [39] Perdew J P, Burke K and Ernzerhof M 1996 *Phys. Rev. Lett.* **77** 3865
- [40] Yankowitz M, Xue J, Cormode D, Sanchez-Yamagishi J D, Watanabe K, Taniguchi T, Jarillo-Herrero P, Jacquod P and LeRoy B J 2012 *Nat. Phys.* **8** 382
- [41] Guo Q, Zhong Y, Huang M, Lu S and Yu Y 2020 *Thin Solid Films* **693** 137709
- [42] Chen H Y, Chen L, Lin J, Tan K L and Li J 1997 *Inorg. Chem.* **36** 1417
- [43] Chen X Q, Li Z, Bai Y, Sun Q, Wang L Z and Dou S X 2015 *Chem. Eur. J.* **21** 1055
- [44] Riha S C, Johnson D C and Prieto A L 2011 *J. Am. Chem. Soc.* **133** 1383